Nanoscale Architectural Control and Macromolecular Engineering of Nonlinear Optical Dendrimers and Polymers for Electro-Optics†

Jingdong Luo,§ Marnie Haller,§ Hong Ma,§ Sen Liu,§ Tae-Dong Kim,§ Yanqing Tian,§ Baoquan Chen,§ Sei-Hum Jang,§ Larry R. Dalton,‡ and Alex K.-Y. Jen*,§,‡

Department of Materials Science & Engineering and Department of Chemistry, University of Washington, Seattle, Washington 98195

Received: September 11, 2003; In Final Form: April 12, 2004

Recent progress in developing highly efficient nonlinear optical dendrimers and polymers for high-performance electro-optic (EO) devices has been reviewed. Our efforts are focused on using nanoscale architectural control to tailor the size, shape, conformation, and functionality of NLO chromophores and macromolecules and studying their effects on poling efficiency. The structures of these materials vary from a 3-D-shaped dendritic chromophore, multifunctional dendrimers with the center core connected to NLO chromophores and cross-linkable functional groups at the periphery, to side-chain-dendronized NLO polymers. All the poling results from these systems have shown dramatically enhanced EO properties (a factor of 2−3) compared to conventional NLO polymers.

Introduction

Organic and polymeric second-order nonlinear optical (NLO) materials have been intensively studied in the past decade for their potential in high-speed electro-optic (EO) devices with very broad bandwidth (up to 200 GHz) and low driving voltages (<1 V).[1,2] One of the most challenging tasks in this area of research is how to translate high molecular nonlinearities ($\mu\beta$) into large macroscopic EO activities (r_{33}) in poled polymers.[2,3] Over the past several years, the concept of using shape modifications on NLO chromophores to improve poling efficiency has been demonstrated to somewhat alleviate the problem of electrostatic interactions.[3] However, these results only provide moderate improvements on EO properties, and the full potential of organic NLO materials has yet to be realized.

In poled polymers, a chromophore is surrounded by other NLO chromophores and polymer chain segments. During the poling process, the chromophore needs to overcome the strong intermolecular electrostatic interactions among chromophores as well as the restriction of polymer chain entanglement on its reorientation along the direction of the electric field. Thus, it is possible to improve the poling efficiency of NLO polymers if the chromophore in the polymer matrix can be structurally shielded from its neighboring chromophores to minimize dipole−dipole interactions. Another promising approach is to create a nanoscale macromolecular ordering, which can lead to a smaller hindrance to reorient NLO chromophores. Until recently, exploratory research for these two possibilities had not been launched, mainly due to a lack of structural and/or shape control in conventional polymer systems with NLO chromophores. Encouragingly, in the past two decades, the ability to control several critical dendrimer design parameters, such as size, shape, surface chemistry, flexibility, and topology, has been explored to provide well-defined, dendritic architectures.[4,5] Since the globular geometry of dendrimers is also well-suited for modifying chromophores to the ideal spherical shape, we have recently employed the dendritic structures to modify NLO chromophores and polymers and systematically investigated the role of the site-isolation effect in determining the material properties.[6−9] Our efforts are focused on tuning the macromolecular architecture of polymeric EO materials from the shape of a flattened sphere, or an umbrella, to a cylinder and studying their effects on poling efficiency. Here we highlight our research progress in the design, synthesis, and properties of different NLO material systems for this purpose. The structures of these materials vary from a 3-D-shaped dendritic chromophore, a multifunctional dendrimer with the center core connected to NLO chromophores and cross-linkable functional groups at the periphery, to side-chain-dendronized NLO polymers. All the poling results from these systems have shown dramatically enhanced EO properties (a factor of 2−3) compared to the conventional NLO polymers.

Experimental Section

General Method. Dichloromethane (CH_2Cl_2) was distilled over phosphorus pentaoxide under nitrogen. Tetrahydrofuran (THF) was distilled from sodium benzophenyl ketyl under nitrogen prior to use. 4-(Dimethylamino)-pyridinium 4-toluenesulfonate (DPTS) was prepared according to the ref 10. The synthesis of **1**−**7** has been previously reported by this research laboratory,[6−9] and the synthesis of **8**, **9**, **14**, and **16** will be reported elsewhere. All other chemicals were purchased from Aldrich unless otherwise specified.

The general procedure for the preparation of compounds **10**, **11**, and **12** is shown in Scheme 1.

Preparation of Compound 10. A mixture of compound **8** (0.85 g, 1.36 mmol), **9** (0.94 g, 4.31 mmol, 3 equiv), and DPTS (0.32 g, 1.08 mmol) was stirred in 50 mL of CH_2Cl_2 for 15 min. DCC (1.07 g, 5.18 mmol) was added, and the reaction mixture was allowed to stir at room temperature for 20 h. After filtration, all the solvent was evaporated under reduced pressure. The crude product was purified by column chromatography using ethyl acetate/hexane (1:1 to 3:2, v/v) as the gradient eluent

† Part of the special issue "Alvin L. Kwiram Festschrift".
§ Department of Materials Science & Engineering.
‡ Department of Chemistry.

10.1021/jp036714o CCC: $27.50
Published on Web 05/21/2004

SCHEME 1: Synthesis of Taper-Shaped Dendritic CLD-type Chromophore 5

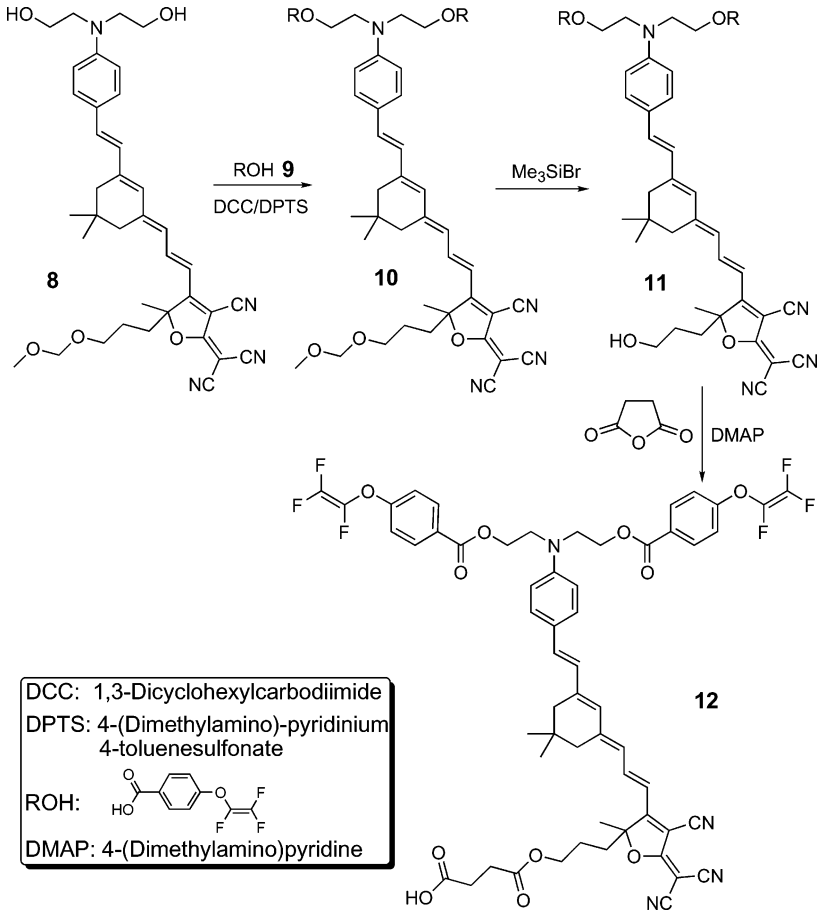

to afford **10** as a blue-greenish oil (0.93 g, 67%). $R_f = 0.4$ (silica gel, ethyl acetate/hexane = 3:2). ^{1}H NMR ($CDCl_3$, TMS, ppm): δ 8.00 (d, $J = 8.8$ Hz, 4H), 7.40 (d, $J = 8.4$ Hz, 2H), 7.12 (d, $J = 8.3$ Hz, 3H), 6.68−6.95 (m, 4H), 6.06−6.53 (m), 4.59 (s, 2H), 4.53 (t, $J = 6.2$ Hz, 4H), 3.85 (t, $J = 6.6$ Hz, 4H), 3.51 (t, $J = 5.9$ Hz, 2H), 3.35 (s, 3H), 2.26−2.55 (m, 4H), 1.15−2.23 (m), 1.06 (s, 6H). Anal. Calcd for $C_{55}H_{50}F_6N_4O_9$: C, 64.45; H, 4.92. Found: C, 64.28; H, 4.87.

Preparation of Compound 11. To a cooled solution of compound **10** (0.93 g, 0.91 mmol) in CH_2Cl_2 under the protection of nitrogen was added dropwise 2.5 mL (18.9 mmol) of bromotrimethylsilane. The reaction mixture was allowed to stir at −30 °C for 4.5 h and was then neutralized with 50 mL of aqueous solution that was saturated with sodium bicarbonate. The residue was extracted with CH_2Cl_2, and the combined extracts were dried over sodium sulfate. The crude product was purified by flash chromatography using ethyl acetate/hexane (3:2 to 2:1, v/v) as the gradient eluent to obtain **11** as a blue-greenish solid (0.38 g, 82%) and retrieve 0.45 g of **10**. $R_f = 0.3$ (silica gel, ethyl acetate/hexane = 2:1). ^{1}H NMR ($CDCl_3$, TMS, ppm): δ 8.01 (d, $J = 8.8$ Hz, 4H), 7.40 (d, $J = 8.4$ Hz, 2H), 7.12 (d, $J = 8.3$ Hz, 3H), 6.68−6.95 (m, 4H), 6.06−6.53 (m), 4.52 (t, $J = 6.2$ Hz, 4H), 3.85 (t, $J = 6.6$ Hz, 4H), 3.51 (t, $J = 5.9$ Hz, 2H), 2.26−2.55 (m, 4H), 1.15−2.23 (m), 1.06 (s, 6H). Anal. Calcd for $C_{53}H_{46}F_6N_4O_8$: C, 64.89; H, 4.73. Found: C, 64.75; H, 4.67.

Preparation of Compound 12. To a solution of compound **11** (0.30 g, 0.31 mmol), pyridine (0.10 mL), and DMAP (0.037 g, 0.31 mmol) in 10 mL of CH_2Cl_2 was added 0.046 g of succinic anhydride (0.46 mmol). After stirring overnight at room temperature, the solution was sequentially washed with 60 mL of 0.5 N HCl solution, and 80 mL of brine, and dried over sodium sulfate. The crude product was purified by flash column chromatography with a gradient eluent of CH_2Cl_2/acetone (6:1, v/v) to CH_2Cl_2/acetone (3:1, v/v) to afford **12** as a blue-greenish solid (0.27 g, 81%). $R_f = 0.30$ (silica gel, ethyl acetate/hexane = 2:1). ^{1}H NMR ($CDCl_3$, TMS, ppm): δ 8.01 (d, $J = 8.8$ Hz, 4H), 7.40 (d, $J = 8.8$ Hz, 2H), 7.10 (d, $J = 8.3$ Hz, 3H), 6.68−6.95 (m, 4H), 6.06−6.53 (m), 4.35 (t, $J = 6.2$ Hz), 4.12 (m, 2H), 3.86 (t, 4H), 2.53−2.91 (m, 4H), 2.26−2.52 (m, 4H), 1.15−2.23 (m), 1.06 (s, 6H). Anal. Calcd for $C_{57}H_{50}F_6N_4O_{11}$: C, 63.33; H, 4.66; N, 5.18. Found: C, 63.45; H, 4.58; N, 5.09.

The general procedure for the preparation of compound **15** is shown in Scheme 2.

Preparation of Side-Chain-Dendronized NLO Polymer 15. To a solution of **12** (0.25 g, 0.231 mmol), poly(4-vinylphenol) (**13**, 0.070 g, 0.58 mmol), and DPTS (0.020 g, 0.068 mmol) in a mixture of 10 mL of THF and 5 mL of CH_2Cl_2 was added 0.060 g of DCC (0.29 mmol). The reaction mixture was allowed to stir at room temperature for 12 h under nitrogen. Then 0.094 g of compound **14** (0.43 mmol), 0.020 g of DPTS (0.068 mmol), and 0.090 g of DCC (0.44 mmol) were added and stirred at room temperature for 24 h. The trace amount of residual phenol was terminated by adding 10 μL of acetic acid and 0.045 g of DCC. Iterative dissolution and filtration removed most of the resultant urea. The filtered CH_2Cl_2 solution was then added dropwise to the stirred methanol. The precipitate was collected after being stirred in methanol for 2 h and reprecipitated by adding dropwise its CH_2Cl_2 solution into methanol to afford polymer **15** as a blue-greenish solid (0.27 g, yield ~78%). ^{1}H NMR ($CDCl_3$, TMS, ppm): δ 7.99 (br d), 7.37 (br s), 5.82−

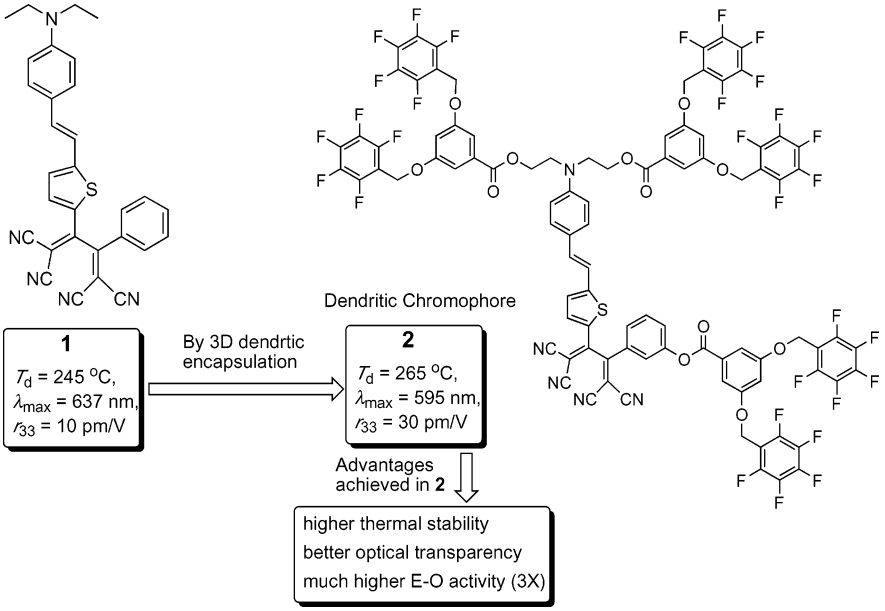

Figure 1. Property comparison between dendritic chromophore **2** and its pristine phenyl-tetracyanobutadienyl (Ph-TCBD) thiophene-stilbene-based NLO chromophore **1**. T_d: the initial decomposition temperature determined by seal-pan differential scanning calorimetry (DSC) at 10 °C/min under nitrogen. APC: amorphous polycarbonate (APC) {poly[bisphenol A carbonate-*co*-4,4′-(3,3,5-trimethylcyclohexylidene)diphenol carbonate}. Electro-optic coefficient (r_{33}) obtained in APC matrix with 12 wt % of core chromophore density by contact poling.

SCHEME 2: Synthesis of Side-Chain-Dendronized Polymer P1

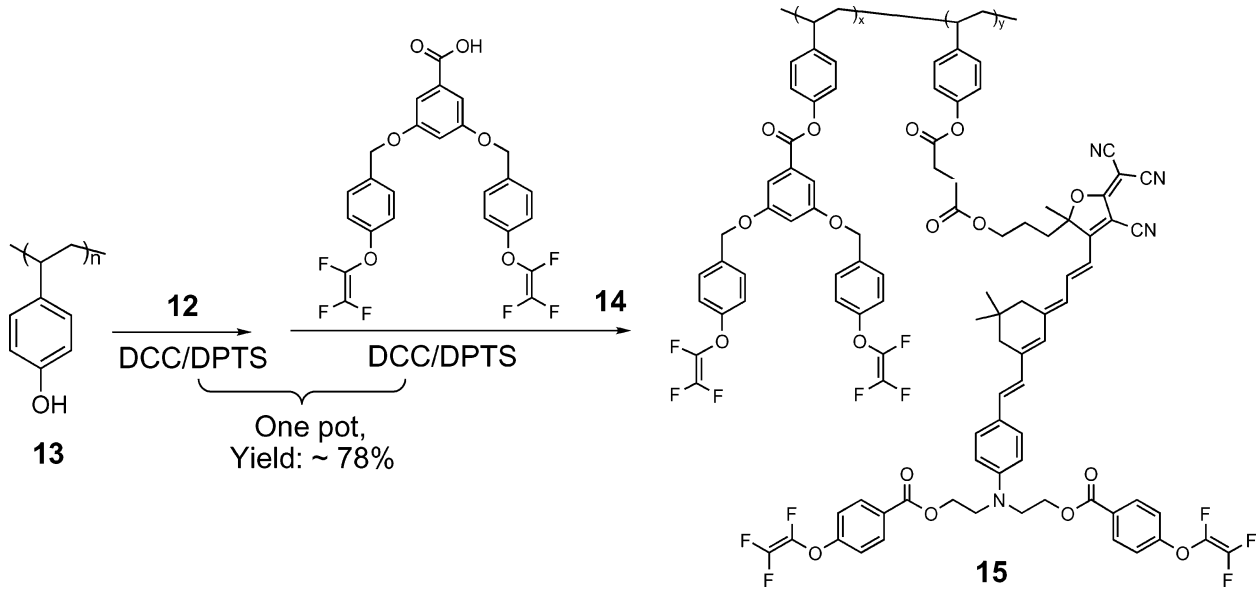

7.18 (br m), 4.73−5.15 (br m), 4.50 (br s), 4.03 (br s), 3.83 (br s), 0.45−3.05 (br m). ^{19}F NMR ($CDCl_3$, C_6F_6, ppm): −136.8∼135.9 (br m), −135.4 (dd, J = 61 Hz), −127.1 (dd, J = 97.7 Hz), −126.8 (br s), −126.4 (br s), −126.0 (br s), −120.3 (br m), −120.2 (br s), −120.1 (br s), −119.3 (dd, J = 61 Hz). UV−vis spectrum of thin film: λ_{max} = 650 nm. T_g = 85 °C.

Results and Discussion

1. Dendritic NLO Chromophore.[8] The fluorinated materials are of particular interest among the various NLO polymer systems, given that they exhibit a combination of high thermal stability, chemical inertness, low dielectric constants, and optical transparency. In order to explore the effect of fluoro-rich dendrons on the microenvironments of the dipolar NLO chromophore, we have synthesized a highly fluorinated dendritic NLO chromophore **2** (Figure 1). This dendritic-shaped chromophore has a phenyl-tetracyanobutadienyl (Ph-TCBD) thiophene-stilbene-based NLO chromophore as the center core, which was encapsulated with three highly fluorinated aromatic dendrons.

The resulting dendritic chromophore **2** exhibits appreciably different properties, such as a large blue-shifted absorption λ_{max} (29 to ∼42 nm), a higher thermal stability (20 °C), and a much higher EO activity (3×), compared to the pristine chromophore **1**.

Since both chromophores contain the same NLO active moiety, the blue-shifted λ_{max} of **2** is largely due to the fluoro-rich dendrons with low polarizability, which can provide a very low dielectric constant environment, encapsulating the core chromophore. Moreover, the dendritic chromophore **2** shows exactly the same UV−vis spectrum when it is dispersed in two kinds of significantly different dielectric matrixes: either a

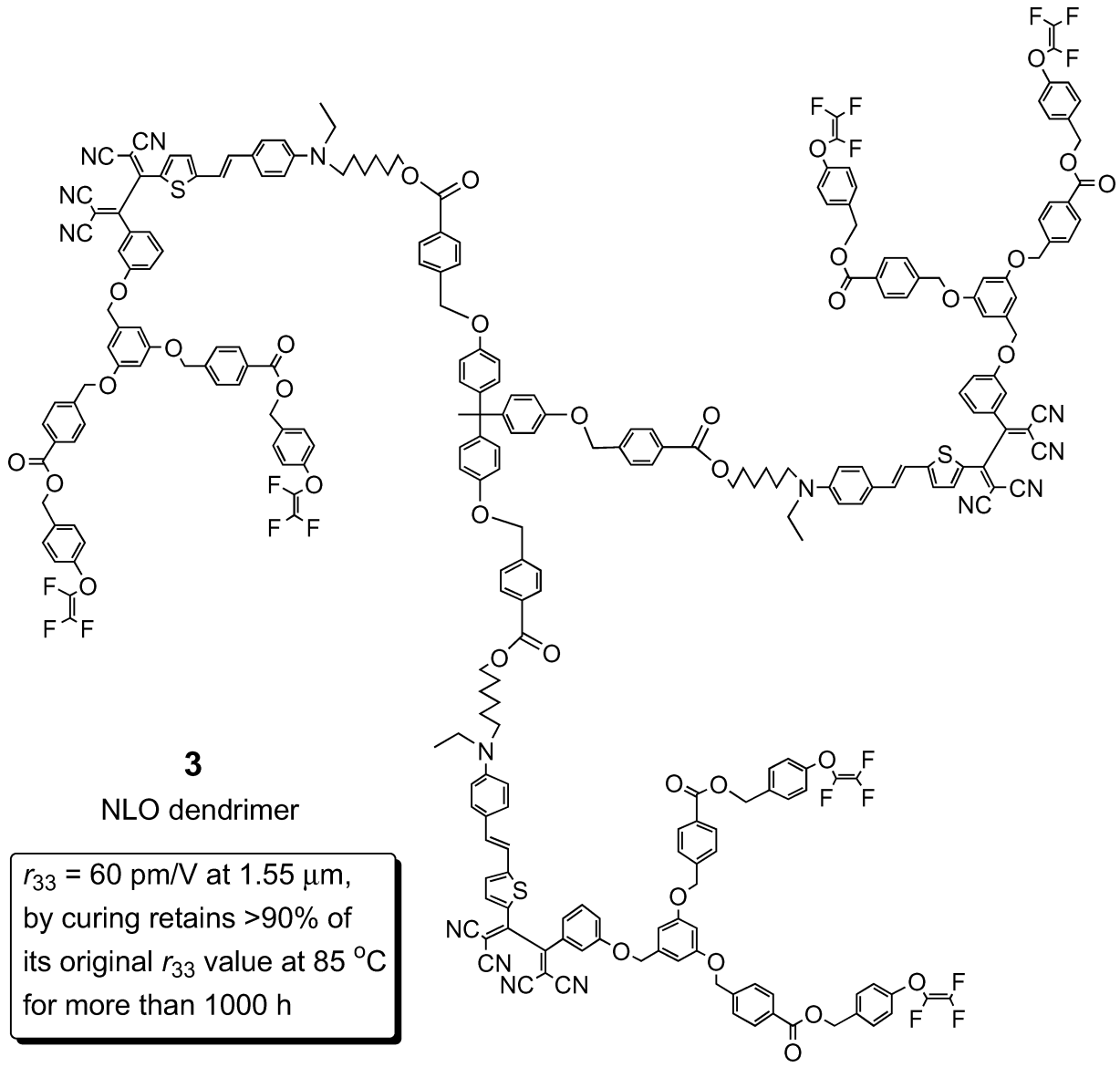

Figure 2. Structure and EO property of a multiarm cross-linkable NLO dendrimer.

nonfluorinated polycarbonate or a highly fluorinated polymer. These results indicate that the fluoro-rich dendrons dominate the microenvironments of the core chromophore in solid films.

More importantly, under a similar poling condition, the poled films of **2** exhibited an r_{33} value of 30 pm/V at 1.3 μm, which is three times higher than that of **1** indicating a significant improvement of poling efficiency. Two major factors related to dendritic modification can contribute to such a significant improvement. The encapsulation of **2** with fluorinated dendrons makes its shape globular-like, which is very close to the ideal spherical shape for achieving the theoretically predicted optimum poling efficiency by the site-isolation effect. Second, because the fluorinated dendrons dominate the microenvironments of the Ph-TCBD chromophore in the solid state, the chromophores are site isolated; therefore, the intermolecular electrostatic interactions are significantly reduced. This, in turn, ameliorates the molecular orientation during the poling process.

The blue-shifted absorption and high C−F content in **2** also contributes to the material's low optical loss at both 1.3 and 1.55 μm, the two major telecommunication operation wavelengths. From the photothermal deflection spectroscopy (PDS), the optical losses of the materials induced by the intrinsic absorption of **2** in polycarbonate are only 0.65 and 0.85 dB/cm at 1.3 and 1.55 μm, respectively. With regard to the relatively high C−H content in the polycarbonate matrix, the major contribution of these loss values are thought to be derived from the matrix itself instead of from **2**. This indicates that this type of highly fluorinated dendritic chromophore has an intrinsic loss much lower than 1 dB/cm and can be considered as a very promising candidate for photonic applications.

2. Cross-Linkable NLO Dendrimers.[9] The above model study provides a clear explanation about how the dendritic effect enhances EO activities. In order to create a structurally more well-defined and thermally more stable NLO material, we have constructed a chromophore-containing dendrimer with multiple NLO chromophore building blocks placed into a precisely designed molecular architecture with predetermined chemical compositions.

NLO dendrimer **3** (Figure 2) was constructed through a double-end functionalization of NLO chromophore **1** as the core and cross-linkable trifluorovinyl ether-containing dendrons as the exterior moieties. Spatial isolation from the dendrimer shell significantly decreases chromophore−chromophore electrostatic interactions, thus enhancing macroscopic optical nonlinearity. Through a sequential hardening/cross-linking process during the electric field poling, a very large EO coefficient (r_{33} = 60 pm/V

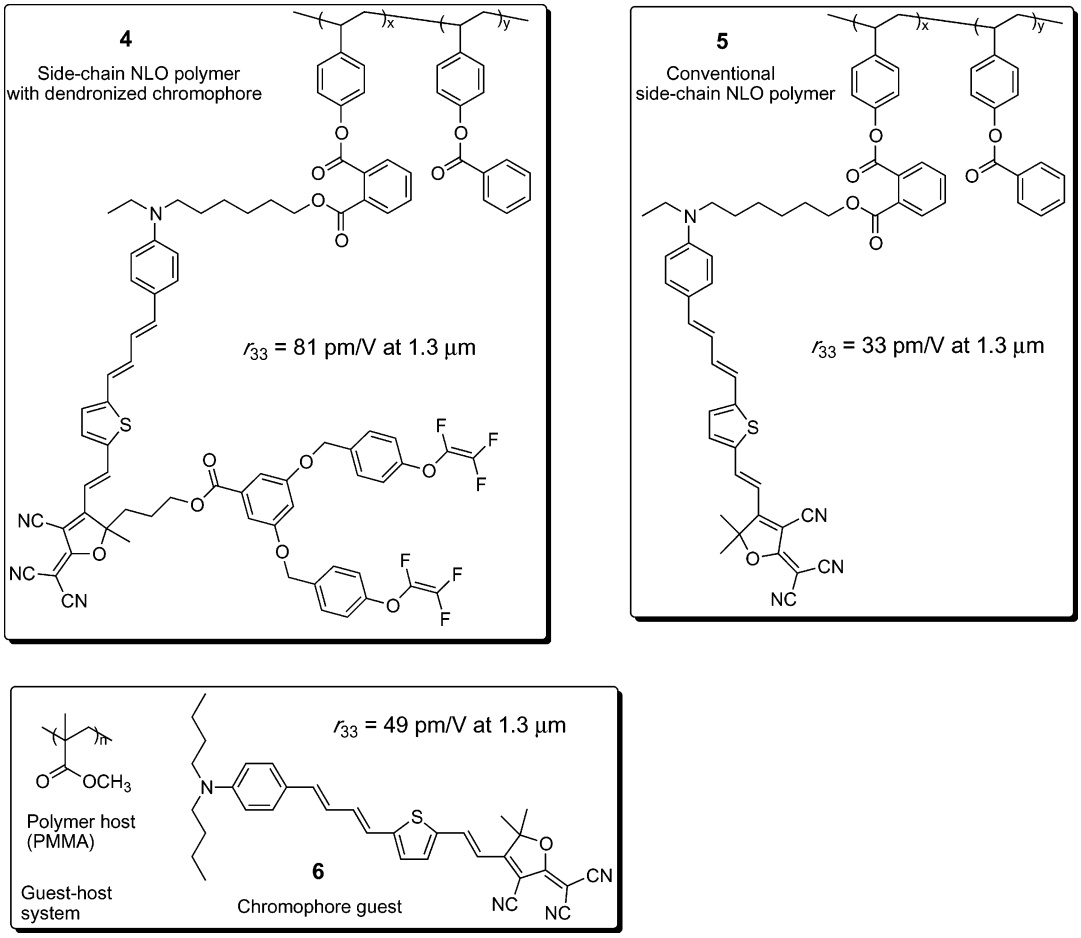

Figure 3. Property comparison between side-chain NLO polymers **4** with dendronized chromophore and conventional side-chain (**5**) or guest−host (**6**/PMMA) systems containing similar chromophores.

at 1.55 μm) and long-term alignment stability (retaining >90% of its original r_{33} value at 85 °C for more than 1000 h) were achieved for this poled dendrimer.

For comparison, EO studies were performed on a guest−host system, in which chromophore **1** without dendron modification (optimized loading level: 30 wt %) was formulated into a high-temperature polyquinoline (PQ-100). This guest−host system showed a much smaller EO coefficient (less than 30 pm/V) and lower temporal stability (it only retained <65% of its original r_{33} value at 85 °C after 1000 h). On the basis of this comparison as well as the systematic model study for dendritic chromophore **2**, the large r_{33} of the poled dendrimer **3** is due to the dendritic effect that allows the NLO dendrimer to be efficiently aligned.

3. Side-Chain NLO Polymers with Dendronized Chromophores.[7] To further optimize EO material properties, a series of hybrid dendritic NLO polymers have been recently developed. This study is to take advantage of the synthetic simplicity and good processability offered by linear polymers and the excellent site-isolation effect provided by dendrimers.

The first side-chain polymer **4**, with a dendronized chromophore, is illustrated in Figure 3. The poled film of **4** (contact poling) showed a very large EO coefficient (r_{33} = 81 pm/V at 1.3 μm). This EO activity is significantly higher than those obtained from the pristine side-chain polymer **5** and the guest−host polymer system (**6**/PMMA) with the same chromophore loading level. The medium EO coefficients from the poled films of **5** and **6**/PMMA indicate that strong chromophore−chromophore electrostatic interactions severely limit the attainable EO activities in ordinary NLO polymeric systems without effective site-isolation moieties. Although several other factors, such as conductivity of the samples and different matrix polymers may also affect the EO activities of the materials, the contribution of these factors to the above difference can be limited to a minor scale through the following systematic study. In both side-chain polymers **4** and **5**, the same polystyrene-based backbone and poling electric fields were utilized. However, the r_{33} value of the side-chain-dendronized NLO polymer **4** is ~2.5 times higher than that of the pristine side-chain NLO polymer **5**. Therefore, the high poling efficiency obtained in the poled film of **4** is mainly due to better site isolation that allows the chromophores to be spatially well distributed and efficiently reorientated. This result is also consistent with the excellent poling behaviors obtained from both the EO dendrimer and the dendritic NLO chromophore doped polymer previously described.

When this new molecular engineering concept was applied to a more efficient NLO molecule (a CLD-type chromophore), extremely large EO coefficients (r_{33} = 97 pm/V at 1.3 μm) were achieved from the poled side-chain-dendronized NLO polymer **7** (Figure 4). These values are also twice superior to those reported from the CLD-based guest−host EO polymer systems, resuming the high poling efficiency of all the dendron-containing NLO materials mentioned above.

In terms of thermal stability, this type of side-chain NLO polymer also shows very encouraging results. We have recently developed a high-T_g cardo-type polyimide with a dendronized CLD-type chromophore.[7b] The poled films of this polymer exhibit the combined advantages of both high poling efficiency and excellent thermal stability. The same high poling efficiency

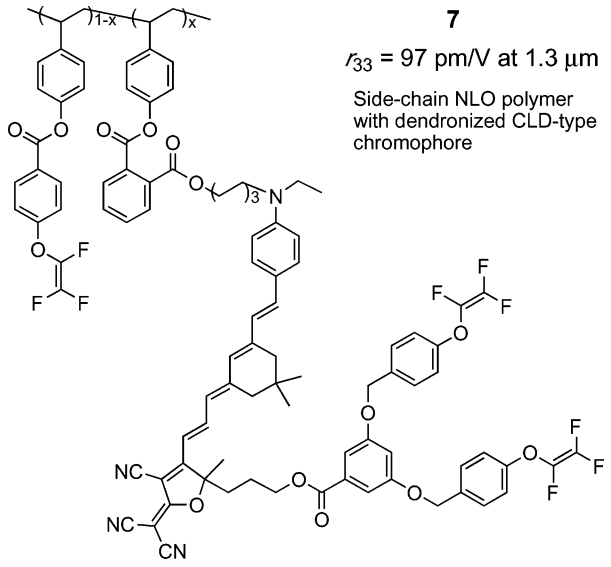

Figure 4. Structure and EO property of side-chain NLO polymer with a dendronized CLD-type chromophore.

through the site-isolation effect has been achieved to afford a very large electro-optic coefficient (71 pm/V at 1.3 μm); more than 90% of this value can be maintained at 85 °C for more than 600 h.

4. Cylindrically Shaped Side-Chain-Dendronized NLO Polymers. It has been demonstrated previously by Percec and Schlüter et al. that well-organized macromolecular cylinders can be achieved by self-assembling of densely loaded flat-tapered dendritic moieties along a linear polymer backbone.[4,5] Inspired by their results, we have designed and synthesized two side-chain-dendronized polymers **15** and **16** (Figure 5) with dendritic-shaped NLO chromophores and fluorinated dendrons as the pendant groups. Polymers **15** and **16** have similar CLD-type chromophores, and their chromophore contents were normalized to 20 wt %. These were calculated by the relative integration of the corresponding characteristic peak in their NMR spectra and further proved by the quantitative analysis of their UV−vis spectra in 1,4-dioxane.

We have introduced some structural differences between **15** and **16** for parallel comparison. Polymer **15** is fully incorporated with flat-tapered side chains along the backbone of polystyrene, and the self-assembling and/or steric congestion of these voluminous dendritic moieties allows us to achieve a psuedocylindrical polymer conformation (Figure 6). Polymer **16** can be considered as a random-coil polymer, since the side-chain chromophores in **16** were introduced as smaller sized and rigid-rod-type conjugated molecules without any shape modification. The property study of **15** and **16** can provide us some insight into how the shape of the side-chain chromophores can affect the performance of the polymers.

Both polymers **15** and **16** possess good solubility in common organic solvents, such as dichloromethane, THF, and cyclopentanone. Their high molecular weights endow the polymers with excellent film-forming properties. However, thermal analysis by differential scanning calorimetry (DSC) shows only one typical glass transition behaviors around 85 °C for **15** (Figure 7) but two transition temperatures for **16** around 65 °C and 85 °C, respectively. This indicates that there may be some significant differences in phase-related transition behaviors between polymers **15** and **16**. We thus performed a very detailed investigation on their EO properties.

For EO measurements, a solution of polymer **15** or **16** in cyclopentanone (13% w/w, filtered through a 0.2 μm syringe filter) was spin-coated onto indium tin oxide (ITO) glass substrates. The films were baked under vacuum at 85 °C overnight to ensure removal of the residual solvent. Then, a thin layer of gold was sputtered onto the films as the top electrode for performing the high electric field poling.

The films of **15** were poled with a DC electric field of 1.15 MV/cm. The r_{33} value was measured using a simple reflection technique at 1.3 μm[11] and showed a very large EO coefficient (r_{33} = 111 pm/V). This value is almost twice as large as those reported from the same CLD-based chromophore in the guest−host EO polymer systems. It is also superior to the value of 97 pm/V obtained from a flexible side-chain polymer **7** with dendronized chromophores,[4b] indicating the exceptionally high poling efficiency was achieved in **15**.

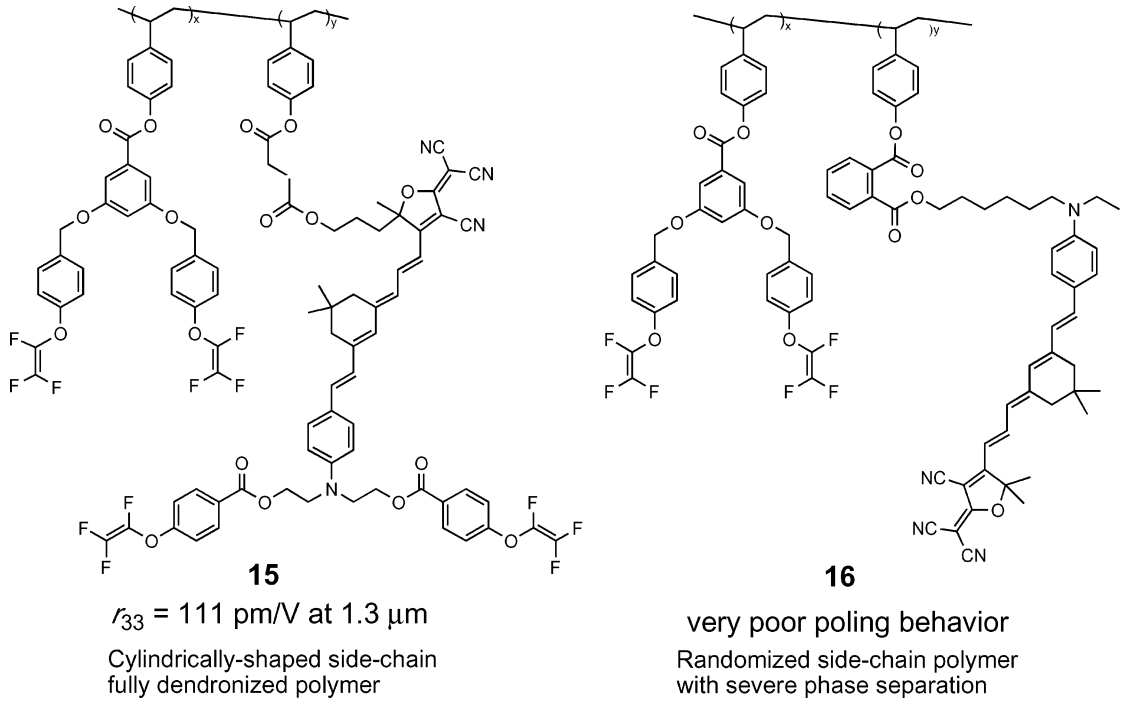

Figure 5. Comparison between a fully side-chain-dendronized polymer **15** and severely phase-separated polymer **16** with CLD-type chromophores.

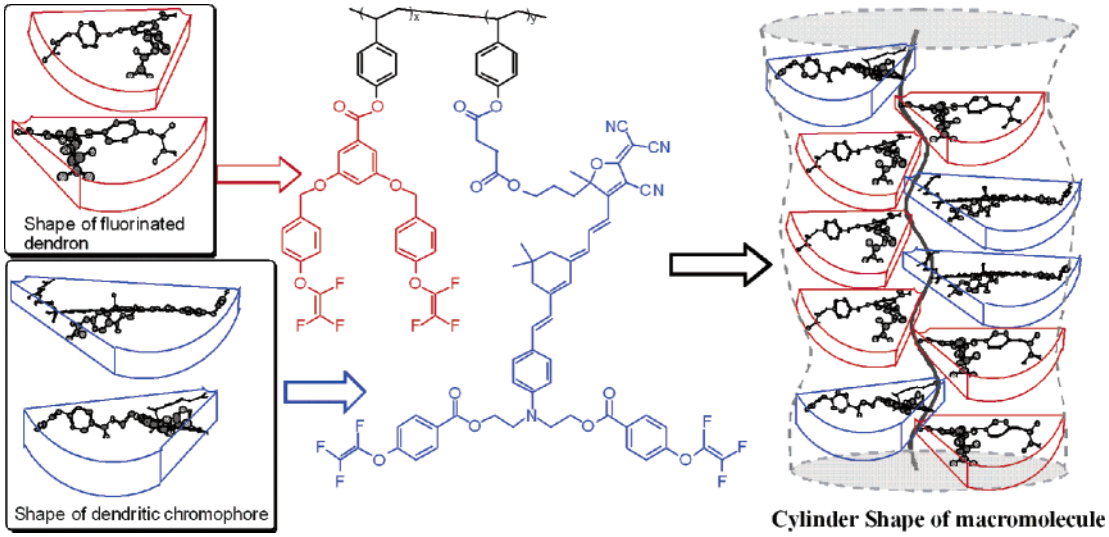

Figure 6. Hypothesis of the site-isolation effect in cylinder-like dendronized NLO polymer **15**: the shape of the dendron and dendritic chromophore is determined by the MOPAC package in CS ChemBats3D.

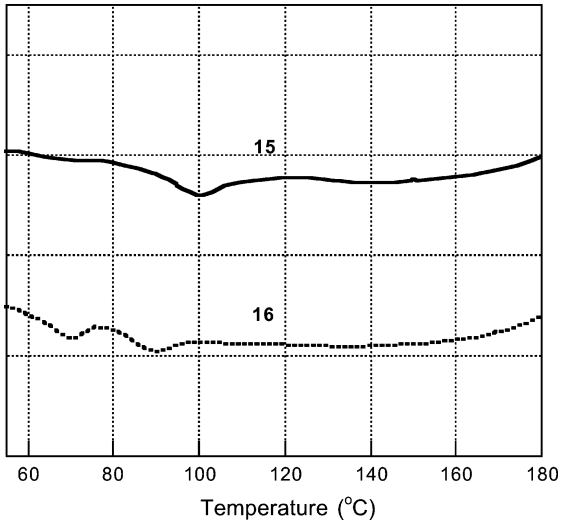

Figure 7. Thermal analysis for polymers **15** and **16** by differential scanning calorimetry (DSC) at 10 °C/min under nitrogen.

However, the poling of **16** was surprisingly unsuccessful. The poling temperature of the higher T_g, around 85 °C, severely damaged the film and electrode. When the lower T_g temperature was used around 65 °C, it did not afford any appreciable r_{33} value.

The excellent poling behavior of **15** can be attributed to the densely packed bulky side groups pushing each other and causing the flexible polymer main chain to form a pseudocylindrical rigid rod conformation. The taper-shaped chromophores are expected to be well spatially isolated in the channels of such formed cylindrical structures. Moreover, due to the rigidity of this type of polymer, the commonly observed chain entanglement in linear polymers should also be suppressed. The thin film UV−vis spectrum of **15** exhibits a strong absorption λ_{max} around 650 nm, which is blue-shifted 56 nm compared to that of the previously reported flexible side-chain polymer using the same chromophore. Such a large blue-shift in absorption indicates that the dipolar chromophores have been well-isolated by the low dielectric fluoro-moieties.[8] The poled polymer **15** also shows encouraging thermal stability. Without cross-linking it can still retain more than 90% of its original r_{33} value after several hundred hours at room temperature. All these encouraging results provide us a new approach to molecular engineer the morphology, optical transparency, and material properties to an unprecedented level.

Polymer **16** is only partially dendronized and is thus a quite randomized polymer. The more flexible side chains of the dipolar chromophores are phase-separated from the side chain of the hydrophobic fluorinated dendrons, verified by its two T_g's in DSC. The lower T_g zone of **16** is believed to be enriched by more flexible chromophoric side chains, and the higher T_g zone is believed to be dominated by closely attached bulky fluoro-dendrons. As a result of severe aggregation between chromophore dipoles, **16** cannot be physically poled by contact poling. The property comparison between **15** and **16** clearly illustrates how the shape of the side-chain chromophores and polymer conformation can determine the material behavior in two wholly different ways.

Conclusion

Compared to the conventional molecular design for organic NLO materials, the concept of using nanoscale architectural control to tailor the size, shape, conformation, and functionality of NLO chromophores and macromolecules provides a great opportunity for simultaneous optimization of macroscopic electro-optic activity, thermal stability, and optical loss. All the results discussed in this review are extremely encouraging, and this new approach may help to launch a new paradigm of molecular engineering for the next generation of high-performance EO materials. Further theoretical investigation and morphology characterization of some of these material systems are ongoing.

Acknowledgment. Financial support from the National Science Foundation (NSF-NIRT and the NSF-STC Program under Agreement Number DMR-0120967) and the Air Force office of Scientific Research (AFOSR) under the MURI Center on Polymeric Smart Skins are acknowledged. Alex K-Y. Jen thanks the Boeing−Johnson Foundation for its support. Tae-Dong Kim thanks the Nanotechnology Center at the University of Washington for the nanotechnology fellowship.

Supporting Information Available: Preparation of 2-[4-(3-{3-[2-(4-{bis-[2-(*tert*-butyl-dimethyl-silanyloxy)-ethyl]-amino}-phenyl)-vinyl]-5,5-dimethyl-cyclohex-2-enylidene}-propenyl)-3-cyano-5-(3-methoxymethoxy-propyl)-5-methy-5*H*-furan-2-

ylidene]-malononitrile, compound **8**, compound **9**, 3,5-bis-(4-trifluorovinyloxy-benzyloxy)-benzoic acid 2,2,2-trichloro-ethyl ester, and compound **14**. This material is available free of charge via the Internet at http://pubs.acs.org.

References and Notes

(1) (a) Shi, Y.; Zhang, C.; Zhang, H.; Bechtel, J. H.; Dalton, L. R.; Robinson, B. H.; Steier, W. H. *Science* **2000**, *288*, 119. (b) Lee, M.; Katz, H. E.; Erben, C.; Gill, D. M.; Gopalan, P.; Heber, J. D.; McGee, D. J. *Science* **2002**, *298*, 1401. (c) Marder, S. R.; Kippelen, B.; Jen, A. K-Y.; Peyghambarian, N. *Nature* **1997**, *388*, 845. (d) Marks, T. J.; Ratner, M. A. *Angew. Chem., Int. Ed. Engl.* **1995**, *34*, 155. (e) Burland, D. M.; Miller, R. D.; Walsh, C. A. *Chem. Rev.* **1994**, *94*, 31.

(2) Kajzar, F.; Lee, K.-S., Jen, A. K-Y. *Adv. Polym. Sci.* **2003**, *161*, 1.

(3) (a) Robinson, B. H.; Dalton, L. R. *J. Phys. Chem. A* **2000**, *104*, 4785. (b) Dalton, L. R.; Steier, W. H.; Robinson, B. H.; Zhang, C.; Ren, A.; Garner, S.; Chen, A.; Londergan, T.; Irwin, L.; Carlson, B.; Fifield, L.; Phelan, G.; Kincaid, C.; Amend, J.; Jen, A. K-Y. *J. Mater. Chem.* **1999**, *9*, 19.

(4) (a) Shu, L.; Schlüter, A. D.; Ecker, C.; Severin, N.; Rabe, J. P. *Angew. Chem., Int. Ed.* **2001**, *40*, 4666. (b) Schlüter, A. D. *Top. Curr. Chem.* **1998**, *197*, 165. (c) Hecht, S.; Fréchet, J. M. J. *Angew. Chem., Int. Ed.* **2001**, *40*, 74. (d) Grayson, S. M.; Fréchet, J. M. J. *Chem. Rev.* **2001**, *101*, 3819. (e) Frey, H. *Angew. Chem., Int. Ed.* **1998**, *37*, 2193. (f) Schlüter, A. D.; Rabe, J. P. *Angew. Chem., Int. Ed.* **2000**, *39*, 864. (g) Ma, H.; Jen, A. K-Y. *Adv. Mater.* **2001**, *13*, 1201.

(5) (a) Percec, V.; Ahn, C. H.; Cho, W. D.; Jamieson, A. M.; Kim, J.; Leman, T.; Schmidt, M.; Gerle, M.; Moeller, M.; Prokhorova, S. A.; Sheiko, S. S.; Cheng, S. Z. D.; Ungar, G. D.; Yeardley, D. J. P. *J. Am. Chem. Soc.* **1998**, *120*, 8619. (b) Percec, V.; Ahn, C. H.; Ungar, G.; Yeardley, D. J. P.; Möller, M.; Sheiko, S. S. *Nature* **1998**, *391*, 161.

(6) Ma, H.; Liu, S.; Luo, J.; Suresh, S.; Liu, L.; Kang, S. H.; Haller, M.; Sassa, T.; Dalton, L. R.; Jen, A. K-Y. *Adv. Funct. Mater.* **2002**, *12*, 565.

(7) (a) Luo, J.; Liu, S.; Haller, M.; Lu, L.; Ma, H.; Jen, A. K-Y. *Adv. Mater.* **2002**, *14*, 1763. (b) Luo, J.; Haller, M.; Li, H.; Tang, H. Z.; Jen, A. K-Y.; Jakka, K.; Chou, C. H.; Shu, C. F. *Macromolecules* **2004**, *37*, 248.

(8) Luo, J.; Ma, H.; Haller, M.; Jen, A. K-Y.; Barto, R. R. *Chem. Commun.* **2002**, 888.

(9) Ma, H.; Chen, B. Q.; Sassa, T.; Dalton, L. R.; Jen, A. K-Y. *J. Am. Chem. Soc.* **2001**, *123*, 986.

(10) Moore J. S.; Stupp, S. I. *Macromolecules* **1990**, *23*, 70.

(11) Teng, C. C.; Man, H. T. *Appl. Phys. Lett.* **1990**, *56*, 1734.